

Structure of high-density amorphous water. II. Neutron scattering study

M.-C. Bellissent-Funel and J. Teixeira

Laboratoire Léon Brillouin,^{a)} CEN-Saclay 91191 Gif-sur-Yvette Cedex, France

L. Bosio

Laboratoire de Physique des Liquides et Electrochimie du CNRS ESPCI, 10 rue Vauquelin, 75231 Paris Cedex 05, France

(Received 21 January 1987; accepted 30 April 1987)

High-density amorphous water is studied by neutron scattering in a Q range extending to 16 \AA^{-1} . The low-density form of amorphous water is also analyzed and compared with previous results. There are very important differences in the composite pair correlation functions of the two forms of amorphous ice, in particular beyond the first nearest-neighbors distance. We conclude that the hydrogen bond network is strongly deformed in a manner analogous to that found in water at high temperature. This is in contrast with the behavior of the pair correlation function of low-density amorphous water, which is closer to that of supercooled water.

I. INTRODUCTION

Previous x-ray measurements of the scattering function of dense amorphous ice¹ have shown that the first neighbor's molecular distance is identical to that found in the low-density form ($\sim 2.80 \text{ \AA}$). On the contrary, beyond this distance, the oxygen-oxygen pair correlation function of high-density amorphous water is completely different from that of the low-density form. The preceding paper² concluded that important distortions of the O-O-O angles are present in the high-density form of amorphous water.

Neutron scattering by water is dominated by the oxygen-deuterium and deuterium-deuterium pair correlation functions. The differences in the structure of the two forms of amorphous ice should appear more directly than in the x-ray measurement, if the main differences come from angular correlations.³

The first determination of the pair correlation function of high-density amorphous ice by neutron scattering has been performed by Floriano *et al.*⁴

In this paper we report on measurements of both forms of amorphous ice as well as a measurement of liquid D_2O at 11°C by neutron scattering. The analysis and interpretation of the data are done in terms of the composite pair-correlation functions.

II. EXPERIMENTAL PROCEDURE

Different samples of the high-density form of D_2O were obtained from crystalline ice I_h , as described by Mishima *et al.*⁵ and in the preceding paper.² The neutron scattering spectra showed some spurious peaks which we attribute to some metastable form of high-pressure crystalline ice. In contrast with the preceding study by x-ray, we were not able to prepare samples completely free of spurious peaks. However, for some of the samples, among the seven we measured during the time allowed for the neutron experiment, the spurious peaks were very weak and easily suppressed in the data processing.

The neutron beam issued from the hot source of reactor Orphée at Saclay and measurements were performed at spectrometer 7C2. We selected an incident wavelength $\lambda = 0.70 \text{ \AA}$ by means of a Cu 111 monochromator. The scattered intensity was measured simultaneously in the total angular range extending up to 180° , with angular steps equal to 0.2° , by using a position-sensitive detector containing 640 cells.⁶ Each spectrum was accumulated for 24 h and the typical number of counts at the first structural peak was around 2×10^6 .

The sample container was a vanadium cylinder 8 mm i.d. and 0.2 mm wall thickness. It was filled with the sample under liquid nitrogen and transferred to a cryostat equipped with a vanadium tail. The temperature in the cryostat was controlled to better than 0.1 K during all the runs. All measurements were performed at 77 K. For each measurement, the temperature was increased until the desired transition was apparent and then reduced to 77 K and kept constant during the run. Independent measurements of the empty cell and of the background were performed and used in the data treatment.

III. DATA ANALYSIS

A. General aspects

The total cross section per molecule $(d\sigma/d\Omega)^{\text{tot}}$, can be separated into five terms: two self terms concern the oxygen and deuterium atoms and three cross terms concern the spatial correlations OO, OD, and DD. The cross terms can be separated in an intra- and an intermolecular part corresponding to correlations between atoms within the same molecule or to atoms belonging to different molecules, respectively;

$$\left(\frac{d\sigma}{d\Omega}\right)^{\text{tot}} = \left(\frac{d\sigma}{d\Omega}\right)^{\text{self}} + \left(\frac{d\sigma}{d\Omega}\right)^{\text{intra}} + \left(\frac{d\sigma}{d\Omega}\right)^{\text{inter}}. \quad (1)$$

Within the static approximation, the self term separates in a coherent part depending on the coherent scattering lengths ($b_O = 0.5805 \times 10^{-12} \text{ cm}$, $b_D = 0.6674 \times 10^{-12} \text{ cm}$) and an incoherent part

^{a)} Laboratoire commun CEA-CNRS.

$$\begin{aligned} \left(\frac{d\sigma}{d\Omega}\right)^{\text{self}} &= \left(\frac{d\sigma}{d\Omega}\right)_{\text{coh}}^{\text{self}} + \left(\frac{d\sigma}{d\Omega}\right)_{\text{inc}}^{\text{self}} \\ &= (b_{\text{O}}^2 + 2b_{\text{D}}^2) + 2\left(\frac{\sigma_i^{\text{D}}}{4\pi}\right), \end{aligned} \quad (2)$$

where σ_i^{D} is the incoherent cross section due to atom D (the incoherent cross section of oxygen is zero).

The intramolecular part of the differential cross section is

$$\begin{aligned} \left(\frac{d\sigma}{d\Omega}\right)^{\text{intra}} &= 4b_{\text{O}}b_{\text{D}}j_0(Qr_{\text{OD}}) \exp(-\gamma_{\text{OD}}Q^2) \\ &\quad + 2b_{\text{D}}^2j_0(Qr_{\text{DD}}) \exp(-\gamma_{\text{DD}}Q^2), \end{aligned} \quad (3)$$

where γ_{OD} and γ_{DD} , appearing in the Debye-Waller factors, are the mean square fluctuations of the distances OD and DD, respectively, and $j_0(x)$ are the spherical Bessel functions.

The intermolecular part is

$$\left(\frac{d\sigma}{d\Omega}\right)^{\text{inter}} = (b_{\text{O}} + 2b_{\text{D}})^2 D_{\text{M}}(Q), \quad (4)$$

where $D_{\text{M}}(Q)$ contains the information on the intermolecular pair correlation function.

It is in general convenient to define the interference function $S_{\text{M}}(Q)$ by

$$S_{\text{M}}(Q) = \left(\frac{d\sigma}{d\Omega}\right)_{\text{coh}} / (b_{\text{O}} + 2b_{\text{D}})^2. \quad (5)$$

From Eqs. (1) and (2) one obtains

$$\begin{aligned} S_{\text{M}}(Q) &= \left[\left(\frac{d\sigma}{d\Omega}\right)_{\text{coh}}^{\text{self}} + \left(\frac{d\sigma}{d\Omega}\right)^{\text{intra}} + \left(\frac{d\sigma}{d\Omega}\right)^{\text{inter}} \right] / \\ &\quad (b_{\text{O}} + 2b_{\text{D}})^2. \end{aligned} \quad (6)$$

The composite pair correlation function $g(r)$ is related to the Fourier transform of $S_{\text{M}}(Q)$:

$$g(r) = 1 + \frac{1}{2\pi^2\rho} \int [S_{\text{M}}(Q) - S_{\text{M}}(\infty)] \frac{\sin Qr}{Qr} Q^2 dQ, \quad (7)$$

where

$$S_{\text{M}}(\infty) = (b_{\text{O}}^2 + 2b_{\text{D}}^2) / (b_{\text{O}} + 2b_{\text{D}})^2. \quad (8)$$

Taking into account Eqs. (2) to (6), it is possible to write

$$S_{\text{M}}(Q) = f_1(Q) + D_{\text{M}}(Q), \quad (9)$$

where $f_1(Q)$ contains the intramolecular and self parts of the interference function

$$\begin{aligned} f_1(Q) &= [b_{\text{O}}^2 + 4b_{\text{O}}b_{\text{D}}j_0(Qr_{\text{OD}}) \\ &\quad \times \exp(-\gamma_{\text{OD}}Q^2) + 2b_{\text{D}}^2j_0(Qr_{\text{DD}}) \\ &\quad \times \exp(-\gamma_{\text{DD}}Q^2)] / (b_{\text{O}} + 2b_{\text{D}})^2. \end{aligned} \quad (10)$$

At very large Q , $D_{\text{M}}(Q)$ goes to zero and $f_1(Q)$ oscillates around the asymptotic value $S_{\text{M}}(\infty) = 0.3347$. At $Q = 0$, $f_1(Q)$ is equal to unity and the interference function $S_{\text{M}}(Q)$ has the thermodynamic limit

$$S_{\text{M}}(0) = \rho k_{\text{B}} T \chi_{\text{T}}, \quad (11)$$

where ρ is the density, k_{B} the Boltzmann constant, T the temperature, and χ_{T} the isothermal compressibility.

B. Data processing

After the usual corrections due to the vanadium container and adsorption, we obtain a spectrum $I(Q)$ which contains both $S_{\text{M}}(Q)$ and the incoherent contribution in an arbitrary scale, together with the inelastic and multiple scattering effects.

It is convenient for the analysis to separate the self and the distinct contributions to $I(Q)$:

$$I(Q) = [I(Q)]^{\text{self}} + [I(Q)]^{\text{dist}}. \quad (12)$$

In order to eliminate the self terms, we used an empirical method.⁷ It assumes that these terms have a smooth Q dependence which can be averaged by some pair function of Q of the form $P(Q) = A - BQ^2 + CQ^4$, where A , B , and C are adjustable constants.

The empirical method has the advantage of taking implicitly into account the inelasticity effects and multiple scattering, assumed to be Q independent for our sample geometry.⁸

We averaged the high Q region of $I(Q)$ by the quadratic polynomial. Then, $I(Q)$ at large Q is an oscillating function around $P(Q)$.

The following step is to Fourier transform the remaining part of $I(Q)$, i.e., $[I(Q)]^{\text{dist}}$. The curve we obtain contains some oscillations below 0.7 Å, which are nonphysical. They can be easily minimized by adjusting the values of the constants A , B , and C .

The final step is the normalization of the data, that is, to relate $I(Q)^{\text{dist}}$ to $S_{\text{M}}(Q)$. For this purpose, we take into account that $S_{\text{M}}(Q)$ has the thermodynamic limit given by Eq. (11) when Q is very small.

Figure 1 gives the $S_{\text{M}}(Q)$ plots for high-density and low-density amorphous ice and for liquid water at 11 °C. The values are tabulated in Table I. Figure 2 shows the weighted functions $4\pi\rho r[g(r) - 1]$ for the same three forms of water.

In order to avoid spurious oscillations due to the limitation of the data to 16 Å⁻¹ we multiplied $[S_{\text{M}}(Q) - S_{\text{M}}(\infty)]$ by the modification function $1/\{\exp[(Q - Q_0)/0.4] + 1\}$ putting $Q_0 = 15$ Å⁻¹.

IV. DISCUSSION

A. Low-density amorphous ice

The interatomic distances, as deduced from the pair correlation function of the low-density form of amorphous ice are identical to that of amorphous ice prepared by vapor deposition on a cold substrate.^{9,10} The main structural peaks are easily identified up to the second-neighbor shell and a deep minimum is observed at 6.5 Å. The pair correlation function shows oscillations extending far beyond these distances (such oscillations are less pronounced for the high-density form). The interatomic distances are very close to those found in an ideal tetrahedral symmetry with the oxygen-oxygen distance around 2.8 Å and the intramolecular distance O-D equal to 0.97 Å. The hydrogen bond distance is close to 1.80 Å showing that each deuterium atom is very close to the alignment O-O. One can remark that this pair correlation function is similar to that of liquid water at low temperatures and, more specifically, to that of supercooled water, as it has been emphasized before.¹¹

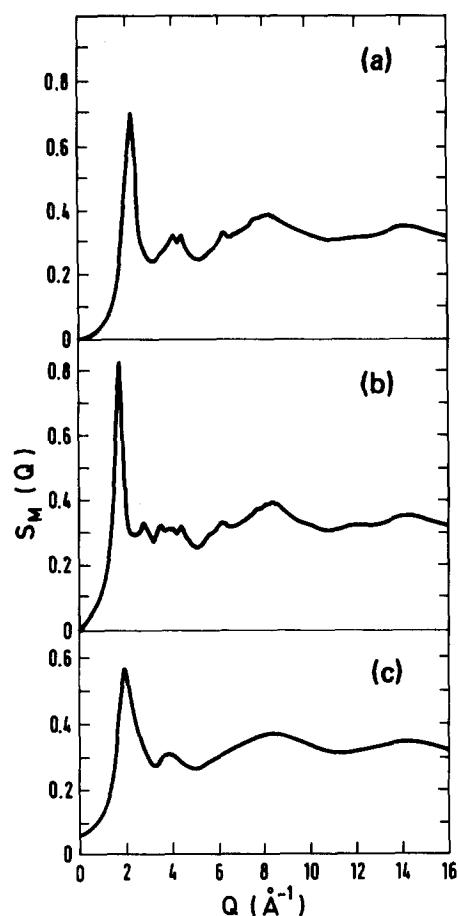


FIG. 1. Molecular structure factor $S_M(Q)$ plotted vs the wave vector Q . (a) High-density amorphous ice. (b) Low-density amorphous ice. (c) Liquid D_2O at 11 °C.

TABLE I. Molecular structure factor $S_M(Q)$ of high-density amorphous ice (HDA), low-density amorphous ice (LDA), and liquid water (LW) at 11 °C.

| Q | $S(Q)$ HD | $S(Q)$ LD | $S(Q)$ LW | Q | $S(Q)$ HD | $S(Q)$ LD | $S(Q)$ LW |
|------|--------------|--------------|--------------|------|--------------|--------------|--------------|
| 0.30 | 0.005 | 0.014 | 0.071 | 7.10 | 0.340 | 0.337 | 0.341 |
| 0.40 | 0.011 | 0.025 | 0.075 | 7.20 | 0.345 | 0.344 | 0.346 |
| 0.50 | 0.011 | 0.031 | 0.083 | 7.30 | 0.351 | 0.348 | 0.350 |
| 0.60 | 0.018 | 0.048 | 0.091 | 7.40 | 0.356 | 0.355 | 0.352 |
| 0.70 | 0.016 | 0.055 | 0.102 | 7.50 | 0.365 | 0.361 | 0.356 |
| 0.80 | 0.025 | 0.069 | 0.114 | 7.60 | 0.376 | 0.372 | 0.362 |
| 0.90 | 0.030 | 0.081 | 0.129 | 7.70 | 0.377 | 0.374 | 0.363 |
| 1.00 | 0.041 | 0.106 | 0.138 | 7.80 | 0.378 | 0.374 | 0.363 |
| 1.05 | 0.042 | 0.117 | 0.144 | 7.90 | 0.382 | 0.378 | 0.367 |
| 1.10 | 0.045 | 0.127 | 0.152 | 8.00 | 0.383 | 0.381 | 0.369 |
| 1.15 | 0.056 | 0.138 | 0.160 | 8.10 | 0.387 | 0.387 | 0.371 |
| 1.20 | 0.070 | 0.150 | 0.170 | 8.20 | 0.386 | 0.388 | 0.370 |
| 1.25 | 0.080 | 0.166 | 0.184 | 8.30 | 0.388 | 0.392 | 0.372 |
| 1.30 | 0.085 | 0.191 | 0.202 | 8.40 | 0.388 | 0.394 | 0.372 |
| 1.35 | 0.095 | 0.232 | 0.220 | 8.50 | 0.381 | 0.389 | 0.369 |
| 1.40 | 0.109 | 0.290 | 0.240 | 8.60 | 0.379 | 0.387 | 0.370 |
| 1.45 | 0.124 | 0.364 | 0.265 | 8.70 | 0.372 | 0.381 | 0.366 |
| 1.50 | 0.135 | 0.458 | 0.298 | 8.80 | 0.369 | 0.375 | 0.363 |
| 1.55 | 0.147 | 0.577 | 0.335 | 8.90 | 0.365 | 0.369 | 0.362 |
| 1.60 | 0.167 | 0.705 | 0.375 | 9.00 | 0.359 | 0.361 | 0.359 |
| 1.65 | 0.195 | 0.802 | 0.416 | 9.10 | 0.356 | 0.355 | 0.357 |
| 1.70 | 0.226 | 0.826 | 0.458 | 9.20 | 0.353 | 0.349 | 0.354 |

TABLE I (continued).

| Q | $S(Q)$ HD | $S(Q)$ LD | $S(Q)$ LW | Q | $S(Q)$ HD | $S(Q)$ LD | $S(Q)$ LW |
|------|--------------|--------------|--------------|-------|--------------|--------------|--------------|
| 1.75 | 0.260 | 0.771 | 0.497 | 9.30 | 0.351 | 0.345 | 0.352 |
| 1.80 | 0.300 | 0.667 | 0.531 | 9.40 | 0.348 | 0.342 | 0.350 |
| 1.85 | 0.349 | 0.558 | 0.555 | 9.50 | 0.345 | 0.339 | 0.348 |
| 1.90 | 0.406 | 0.469 | 0.569 | 9.60 | 0.341 | 0.335 | 0.345 |
| 1.95 | 0.472 | 0.404 | 0.570 | 9.70 | 0.337 | 0.332 | 0.340 |
| 2.00 | 0.544 | 0.358 | 0.562 | 9.80 | 0.334 | 0.331 | 0.338 |
| 2.05 | 0.614 | 0.327 | 0.545 | 9.90 | 0.332 | 0.329 | 0.337 |
| 2.10 | 0.667 | 0.310 | 0.524 | 10.00 | 0.331 | 0.327 | 0.334 |
| 2.15 | 0.696 | 0.302 | 0.501 | 10.10 | 0.327 | 0.324 | 0.331 |
| 2.20 | 0.697 | 0.297 | 0.476 | 10.20 | 0.325 | 0.321 | 0.329 |
| 2.25 | 0.670 | 0.294 | 0.453 | 10.30 | 0.321 | 0.317 | 0.326 |
| 2.30 | 0.616 | 0.291 | 0.433 | 10.40 | 0.317 | 0.315 | 0.323 |
| 2.35 | 0.545 | 0.289 | 0.415 | 10.50 | 0.315 | 0.312 | 0.321 |
| 2.40 | 0.475 | 0.290 | 0.400 | 10.60 | 0.313 | 0.310 | 0.319 |
| 2.45 | 0.421 | 0.293 | 0.387 | 10.70 | 0.312 | 0.309 | 0.318 |
| 2.50 | 0.383 | 0.294 | 0.376 | 10.80 | 0.310 | 0.306 | 0.315 |
| 2.55 | 0.354 | 0.295 | 0.366 | 10.90 | 0.312 | 0.308 | 0.316 |
| 2.60 | 0.328 | 0.297 | 0.357 | 11.00 | 0.311 | 0.308 | 0.315 |
| 2.65 | 0.308 | 0.306 | 0.347 | 11.10 | 0.310 | 0.307 | 0.314 |
| 2.70 | 0.296 | 0.318 | 0.338 | 11.20 | 0.311 | 0.310 | 0.315 |
| 2.75 | 0.289 | 0.327 | 0.330 | 11.30 | 0.312 | 0.311 | 0.313 |
| 2.80 | 0.284 | 0.330 | 0.323 | 11.40 | 0.314 | 0.313 | 0.314 |
| 2.85 | 0.279 | 0.327 | 0.316 | 11.50 | 0.315 | 0.316 | 0.315 |
| 2.90 | 0.274 | 0.322 | 0.309 | 11.60 | 0.315 | 0.319 | 0.316 |
| 2.95 | 0.268 | 0.315 | 0.302 | 11.70 | 0.317 | 0.321 | 0.316 |
| 3.00 | 0.262 | 0.305 | 0.295 | 11.80 | 0.318 | 0.322 | 0.318 |
| 3.05 | 0.257 | 0.295 | 0.289 | 11.90 | 0.319 | 0.324 | 0.319 |
| 3.10 | 0.254 | 0.288 | 0.285 | 12.00 | 0.319 | 0.324 | 0.319 |
| 3.15 | 0.254 | 0.282 | 0.282 | 12.10 | 0.320 | 0.325 | 0.321 |
| 3.20 | 0.254 | 0.277 | 0.280 | 12.20 | 0.320 | 0.325 | 0.322 |
| 3.30 | 0.254 | 0.279 | 0.282 | 12.30 | 0.321 | 0.325 | 0.323 |
| 3.40 | 0.262 | 0.303 | 0.292 | 12.40 | 0.321 | 0.325 | 0.324 |
| 3.50 | 0.274 | 0.319 | 0.302 | 12.50 | 0.322 | 0.324 | 0.325 |
| 3.60 | 0.278 | 0.319 | 0.307 | 12.60 | 0.323 | 0.324 | 0.326 |
| 3.70 | 0.285 | 0.310 | 0.309 | 12.70 | 0.322 | 0.323 | 0.328 |
| 3.80 | 0.300 | 0.311 | 0.312 | 12.80 | 0.325 | 0.323 | 0.329 |
| 3.90 | 0.309 | 0.310 | 0.309 | 12.90 | 0.327 | 0.324 | 0.331 |
| 4.00 | 0.321 | 0.312 | 0.304 | 13.00 | 0.329 | 0.326 | 0.333 |
| 4.10 | 0.323 | 0.312 | 0.301 | 13.10 | 0.331 | 0.327 | 0.334 |
| 4.20 | 0.310 | 0.300 | 0.297 | 13.20 | 0.336 | 0.331 | 0.337 |
| 4.30 | 0.308 | 0.302 | 0.291 | 13.30 | 0.338 | 0.333 | 0.339 |
| 4.40 | 0.321 | 0.318 | 0.286 | 13.40 | 0.341 | 0.336 | 0.340 |
| 4.50 | 0.313 | 0.313 | 0.283 | 13.50 | 0.342 | 0.338 | 0.341 |
| 4.60 | 0.290 | 0.294 | 0.276 | 13.60 | 0.345 | 0.341 | 0.343 |
| 4.70 | 0.279 | 0.281 | 0.273 | 13.70 | 0.348 | 0.345 | 0.345 |
| 4.80 | 0.268 | 0.268 | 0.269 | 13.80 | 0.349 | 0.347 | 0.345 |
| 4.90 | 0.261 | 0.260 | 0.267 | 13.90 | 0.351 | 0.350 | 0.346 |
| 5.00 | 0.259 | 0.256 | 0.268 | 14.00 | 0.353 | 0.353 | 0.347 |
| 5.10 | 0.255 | 0.254 | 0.268 | 14.10 | 0.354 | 0.355 | 0.348 |
| 5.20 | 0.255 | 0.256 | 0.272 | 14.20 | 0.353 | 0.355 | 0.348 |
| 5.30 | 0.254 | 0.261 | 0.275 | 14.30 | 0.354 | 0.356 | 0.348 |
| 5.40 | 0.262 | 0.273 | 0.281 | 14.40 | 0.352 | 0.355 | 0.347 |
| 5.50 | 0.271 | 0.285 | 0.286 | 14.50 | 0.353 | 0.355 | 0.347 |
| 5.60 | 0.277 | 0.293 | 0.291 | 14.60 | 0.351 | 0.354 | 0.346 |
| 5.70 | 0.284 | 0.300 | 0.296 | 14.70 | 0.350 | 0.353 | 0.345 |
| 5.80 | 0.289 | 0.303 | 0.299 | 14.80 | 0.349 | 0.351 | 0.344 |
| 5.90 | 0.296 | 0.308 | 0.303 | 14.90 | 0.346 | 0.349 | 0.343 |
| 6.00 | 0.307 | 0.316 | 0.308 | 15.00 | 0.343 | 0.347 | 0.341 |
| 6.10 | 0.321 | 0.326 | 0.312 | 15.10 | 0.341 | 0.344 | 0.340 |
| 6.20 | 0.331 | 0.333 | 0.315 | 15.20 | 0.340 | 0.344 | 0.339 |
| 6.30 | 0.331 | 0.329 | 0.319 | 15.30 | 0.337 | 0.340 | 0.337 |
| 6.40 | 0.321 | 0.318 | 0.320 | 15.40 | 0.335 | 0.338 | 0.335 |
| 6.50 | 0.321 | 0.317 | 0.323 | 15.50 | 0.334 | 0.337 | 0.334 |
| 6.60 | 0.325 | 0.321 | 0.326 | 15.60 | 0.331 | 0.334 | 0.331 |
| 6.70 | 0.328 | 0.324 | 0.327 | 15.70 | 0.329 | 0.332 | 0.329 |
| 6.80 | 0.330 | 0.326 | 0.330 | 15.80 | 0.326 | 0.330 | 0.327 |
| 6.90 | 0.333 | 0.330 | 0.336 | 15.90 | 0.325 | 0.329 | 0.326 |
| 7.00 | 0.338 | 0.335 | 0.338 | 16.00 | 0.334 | 0.334 | 0.334 |

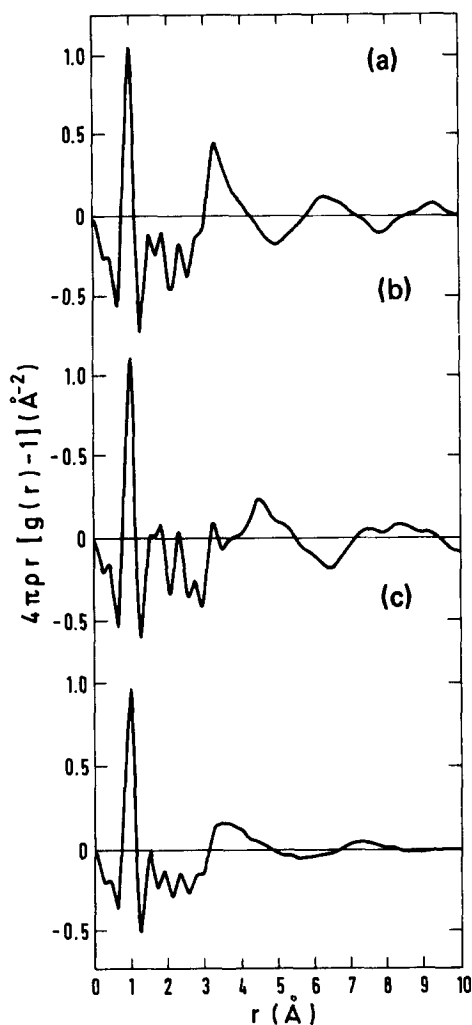


FIG. 2. Pair correlation function, $4\pi r[g(r) - 1]$ plotted vs r . (a) High-density amorphous ice. (b) Low-density amorphous ice. (c) Liquid D_2O at 11 °C.

B. High-density amorphous ice

The pair correlation function of the high-density form of amorphous ice is completely different from that of the low-density form (see Fig. 3 for the comparison). Its general shape is in agreement with the previous results of Floriano *et al.*⁴ A general feature is that all the peaks are broader, showing that interatomic correlations are weaker than in the low-density form. The peak that corresponds to the nearest oxygen–oxygen distance can be seen as a shoulder around 2.8 Å and is in good agreement with the results of the x-ray experiment.² The intramolecular O–D distance is the same (0.97 Å) as that of the low-density form and the intramolecular D–D distance (1.5 Å) appears smaller than in the low-density form.⁹ As a consequence, there is a complete splitting of the composite peak (at 1.75 Å for the low-density form) into two peaks at 1.5 and 1.8 Å (the hydrogen bond distance). This means that the deuterium atoms are not in the O–O alignment and, consequently, that the intramolecular angle DOD is around 106°, that is about 4° smaller than the regular tetrahedral angle. This situation is analogous to that found in liquid water, particularly at high temperature and in the

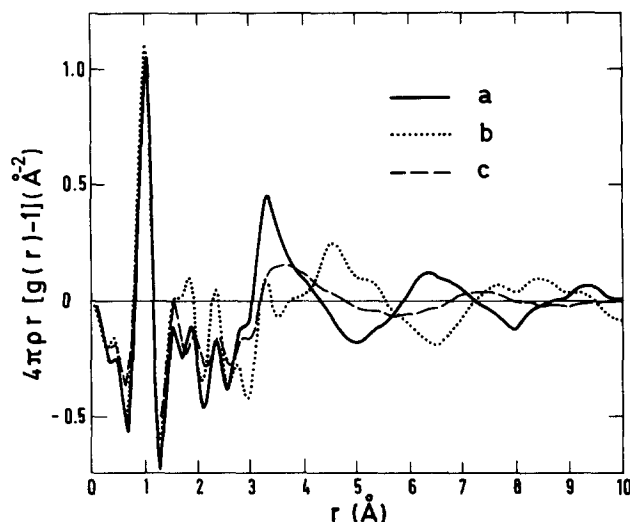


FIG. 3. The same as in Fig. 2 plotted in the same graph for the purpose of comparison. (a) High-density amorphous ice, (b) low-density amorphous ice, (c) liquid D_2O at 11 °C.

vapor phase.¹² Schematically, one can say that, in the high-density form of amorphous ice, the water molecule appears to be more independent and uncorrelated from its neighbors.

Beyond the first nearest-neighbors distance, the two pair correlation functions are very different. For the high-density form, a very broad peak is present at 3.35 Å and a minimum exists at 5.0 Å, i.e., in the region where there is a maximum for the low-density form.

We interpret the pair correlation function of the high-density form of amorphous ice by the loss of the main O–O–O angular correlations. Because the oxygen–oxygen pair correlation function contributes only for 9% of the composite $g(r)$, the peak observed by x-ray around 4.6 Å,² appears only as a small bump. All the distances beyond the first nearest-neighbors distance are reduced. As a consequence, it is impossible to distinguish among different atoms at the level of the second neighbors. They appear as a broad peak around 3.5 Å. The comparison with the pair correlation function of liquid water (see Fig. 2) is, from this point of view, particularly striking. Actually, the behavior of the pair correlation function of dense amorphous ice can be compared with that of liquid water at high temperature. Roughly speaking, the low-density form of amorphous ice appears as the limit for supercooled water. Conversely, the structure of the high-density form suggests that it could be similar to that of high-temperature water after quenching.

It is worth noting that, for the low-density form, the structure present between 4.5 and 6.0 Å is connected to the formation of tetrahedrally coordinated patches, as in supercooled water.¹¹ In contrast, it is clear that such patches are not present in the high-density form, either because the hydrogen bonds are broken, i.e., the molecular interaction energy is, on average, too low or, more likely, because the hydrogen bond network is distorted as in liquid water at high pressures.¹³ This feature explains the high density of this form of amorphous ice, as compared with liquid water. Con-

sequently, it would be probably interesting to compare the pair correlation functions of high-density amorphous ice and that of liquid water at high pressure, as previously suggested,⁴ using neutron scattering techniques.

ACKNOWLEDGMENT

We acknowledge Dr. J. C. Dore for many fruitful discussions.

¹L. Bosio, G. P. Johari, and J. Teixeira, *Phys. Rev. Lett.* **56**, 460 (1986).

²A. Bizid, L. Bosio, A. Defrain, and M. Oumezzine, *J. Chem. Phys.* **87**, 2225 (1987).

³J. C. Dore, in *Water Science Reviews*, edited by F. Franks (Cambridge University, Cambridge, 1985), Vol. 1, Chap. 1.

⁴M. A. Floriano, E. Whalley, E. C. Svensson, and V. F. Sears, *Phys. Rev. Lett.* **57**, 3062 (1986).

⁵O. Mishima, L. D. Calvert, and E. Whalley, *Nature* **310**, 393 (1984); **314**, 76 (1985).

⁶J. P. Ambroise, M.-C. Bellissent-Funel, and R. Bellissent, *Rev. Phys. Appl.* **19**, 731 (1984).

⁷D. G. Montague, I. P. Gibson, and J. C. Dore, *Mol. Phys.* **44**, 1355 (1981); M. Deraman, J. C. Dore, J. G. Powles, J. H. Holloway, and P. Chieux, *ibid.* **55**, 1351 (1985).

⁸V. F. Sears, *Adv. Phys.* **24**, 1 (1975).

⁹A. H. Narten, C. G. Venkatesh, and S. A. Rice, *J. Chem. Phys.* **64**, 1106 (1976).

¹⁰M. R. Chowdhury, J. C. Dore, and J. T. Wenzel, *J. Non-Cryst. Solids* **53**, 247 (1982).

¹¹M.-C. Bellissent-Funel, L. Bosio, J. Dore, J. Teixeira, and P. Chieux, *Eur.ophys. Lett.* **2**, 241 (1986).

¹²W. S. Benedict, N. Gailar, and E. K. Plyler, *J. Chem. Phys.* **24**, 1139 (1956).

¹³G. E. Walrafen, *J. Solution Chem.* **2**, 159 (1973).

The Journal of Chemical Physics is copyrighted by the American Institute of Physics (AIP). Redistribution of journal material is subject to the AIP online journal license and/or AIP copyright. For more information, see <http://ojps.aip.org/jcpo/jcpcr/jsp>
Copyright of Journal of Chemical Physics is the property of American Institute of Physics and its content may not be copied or emailed to multiple sites or posted to a listserv without the copyright holder's express written permission. However, users may print, download, or email articles for individual use.

The Journal of Chemical Physics is copyrighted by the American Institute of Physics (AIP). Redistribution of journal material is subject to the AIP online journal license and/or AIP copyright. For more information, see <http://ojps.aip.org/jcpo/jcpcr/jsp>